AD-A175 291 STRUCTURE AND DYNAMICS OF POLAR CAP F-LAYER PATCHES(U) 1/1
AIR FORCE GEOPHYSICS LAB HANSCOM AFB MA
E J WEBER ET AL 31 MAR 86 AFGL-TR-86-0074

UNCLASSIFIED F/G 4/1 NL

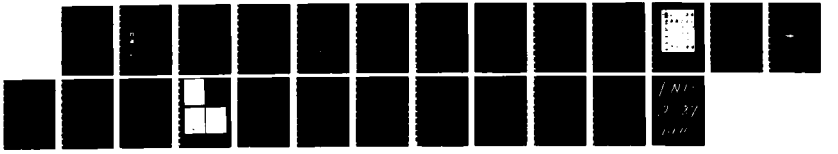

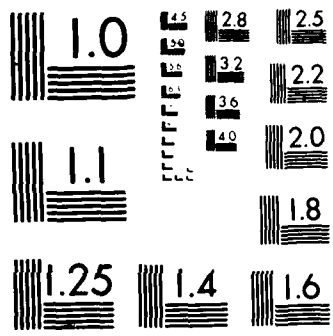

AFGL-TR-86-0074
ENVIRONMENTAL RESEARCH PAPERS, NO. 961

Structure and Dynamics of Polar Cap F-Layer Patches

E.J. WEBER
J.A. KLOBUCHAR
J. BUCHAU
H.C. CARLSON, JR.
R.C. LIVINGSTON
O. de la BEAUJARDIERE
M. McCREADY
J.G. MOORE
G.J. BISHOP

31 March 1986

IONOSPHERIC PHYSICS DIVISION PROJECT 4643
AIR FORCE GEOPHYSICS LABORATORY
HANSCOM AFB, MA 01731

*Original contains color plates: All DTIC reproductions will be in black and white

"This technical report has been reviewed and is approved for publication."

FOR THE COMMANDER

HERBERT C. CARLSON
Branch Chief

ROBERT A. SKRIVANEK
Division Director

This document has been reviewed by the ESD Public Affairs Office (PA) and is releasable to the National Technical Information Service (NTIS).

Qualified requestors may obtain additional copies from the Defense Technical Information Center. All others should apply to the National Technical Information Service.

If your address has changed, or if you wish to be removed from the mailing list, or if the addressee is no longer employed by your organization, please notify AFGL/DAA, Hanscom AFB, MA 01731. This will assist us in maintaining a current mailing list.

Unclassified
SECURITY CLASSIFICATION OF THIS PAGE

REPORT DOCUMENTATION PAGE

1a REPORT SECURITY CLASSIFICATION Unclassified	1b RESTRICTIVE MARKINGS
2a SECURITY CLASSIFICATION AUTHORITY	3 DISTRIBUTION/AVAILABILITY OF REPORT Approved for public release; distribution unlimited.
2b DECLASSIFICATION/DOWNGRADING SCHEDULE	
4 PERFORMING ORGANIZATION REPORT NUMBER(S) ERP, No. 951 AFGL-TR-86-0074	5 MONITORING ORGANIZATION REPORT NUMBER(S)
6a NAME OF PERFORMING ORGANIZATION Air Force Geophysics Laboratory 6b OFFICE SYMBOL (If applicable) LIS	7a NAME OF MONITORING ORGANIZATION
6c ADDRESS (City, State, and ZIP Code) Hanscom AFB Massachusetts 01731	7b ADDRESS (City, State, and ZIP Code)
8a NAME OF FUNDING/SPONSORING ORGANIZATION 8b OFFICE SYMBOL (If applicable)	9 PROCUREMENT INSTRUMENT IDENTIFICATION NUMBER
8c ADDRESS (City, State, and ZIP Code)	10 SOURCE OF FUNDING NUMBERS PROGRAM ELEMENT NO: 62101F PROJECT NO: 4643 TASK NO: 08 WORK UNIT ACCESSION NO: 06

11 TITLE (Include Security Classification)

Structure and Dynamics of Polar Cap F-layer Patches

12 PERSONAL AUTHOR(S) E.J. Weber, J.A. Klobuchar, J. Buchau, H.C. Carlson, R.C. Livingston, O. de la Beaujardiere, M. McCready, J.G. Moore, and G.J. Bishop

13a TYPE OF REPORT	13b TIME COVERED	14 DATE OF REPORT (Year, Month, Day)	15 PAGE COUNT
Scientific Interim	FROM Mar 85 TO Mar 86	1986 March 31	24

16 SUPPLEMENTARY NOTATION

Radio Physics Laboratory, SRI International, Menlo Park, California 94025

17 COSATI CODES			18 SUBJECT TERMS (Continue on reverse if necessary and identify by block number)
FIELD	GROUP	SUB GROUP	Polar cap plasma; Polar cap ionospheric irregularities

19 ABSTRACT (Continue on reverse if necessary and identify by block number)

Coordinated measurements of F-region plasma patches were conducted on 3 and 4 February 1984 from Thule and Sondrestrom, Greenland. Optical, ionosonde, amplitude scintillation, Total Electron Content (TEC), and incoherent scatter radar measurements were combined to reveal several new aspects of the structure and transport of these localized regions of enhanced F-region ionization. These patches were directly tracked for the first time flowing anti-sunward from the center of the polar cap to the poleward edge of the auroral oval. Amplitude scintillation caused by irregularities within these structured patches showed a systematic increase on the trailing edge of the patches consistent with an E × B instability mechanism. Equally important, significant scintillation was also observed on the leading edge and throughout the patch, requiring another instability mechanism to produce irregularities throughout the interior of the patch.

20 DISTRIBUTION/AVAILABILITY OF ABSTRACT	21 ABSTRACT SECURITY CLASSIFICATION
☐ UNCLASSIFIED/UNLIMITED ☒ SAME AS RPT ☐ DTIC USERS	Unclassified
22a NAME OF RESPONSIBLE INDIVIDUAL Edward J. Weber	22b TELEPHONE (Include Area Code) (617) 377-3121
	22c OFFICE SYMBOL AFGL/LIS

DD FORM 1473, 84 MAR 83 APR edition may be used until exhausted
All other editions are obsolete

SECURITY CLASSIFICATION OF THIS PAGE
Unclassified

Preface

The authors would like to thank J. F. Vickrey of SRI International for valuable discussions, and J. Doupnik of Utah State University for access to the radar data that was collected as part of a joint-Sondrestrom-EISCAT experiment. Engineering support from R. W. Gowell, J. W. F. Lloyd, J. B. Waaramaa, and MSgt R. Galik made these measurements possible. Flight support was provided by the 4950th Test Wing, Wright-Patterson Air Force Base, Ohio. This research was partially funded by the following contracts: DNA 599 QMX BC, WU 00103 (with AFGL); AFGL-F19628-84-K-0019 and NSF contractual agreement ATM 81 21671 (with SRI); and AFOSR Task 2310G9 with (AFGL). The authors gratefully acknowledge approval from the Danish Commission for Scientific Research in Greenland to conduct these experiments.

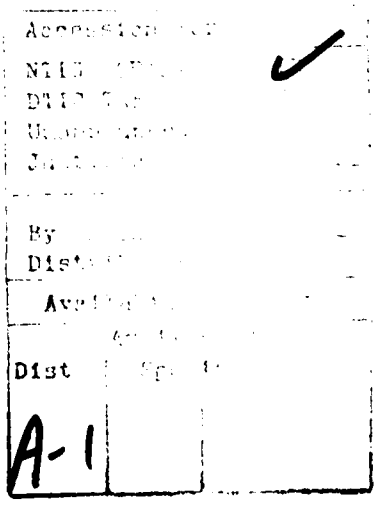

Contents

Illustrations

Tables

Structure and Dynamics of Polar Cap F-layer Patches

1. INTRODUCTION

In recent years, researchers using a variety of measurement techniques have observed patches of enhanced F-region plasma in the polar cap ionosphere. They were first recognized in the central polar cap (86° Corrected Geomagnetic Latitude) during winter using optical and radio wave diagnostics (Buchau et al[1] and Weber et al[2]). These observations led to a description of non-locally produced regions of increased F-region density (factors of 5 to 10 times above background with maximum values of ~ 10^6 el/cm^3 inside the patches) with horizontal dimensions of up to 1000 km. The 6300 Å airglow emission within the patches, which drift in the anti-sunward direction with speeds from 100 to 1000 m/sec, is due to dissociative recombination within the high plasma density region.

Simultaneous satellite amplitude and phase fluctuation measurements (scintillation) showed that the patches are frequently accompanied by small scale (< 1 km) ionospheric irregularities that cause significant scintillation at 250 MHz.

More recent observations in the central polar cap show a diurnal or UT variation of the maximum density within the patches that has been related to a longitudinal

(Received for publication 27 March 1986)

1. Buchau, J., Reinisch, B.W., Weber, E.J., and Moore, J.G. (1983) Structure and dynamics of the winter polar cap F Region, Radio Sci., 18:995.

2. Weber, E.J., Buchau, J., Moore, J.G., Sharber, J.R., Livingston, R.C., Winningham, J.D., and Reinisch, B.W. (1984) F-layer ionization patches in the polar cap, J. Geophys. Res., 89:1683.

variation in the plasma source region. Buchau et al[3] (1985 and references therein) postulated that the patches originate equatorward of the dayside cusp in the solar-produced ionosphere, and are subsequently convected into the polar cap. Thus, the UT variation in the polar cap reflects the variation of geographic latitude of the source region at different longitudes, due to the separation of the geographic and geomagnetic poles. All sky imaging and ionospheric sounding in the polar cap near the dayside cusp have shown the emergence of these patches from the cusp region (Weber and Buchau[4]). Incoherent scatter radar measurements from Sondrestrom (Kelly and Vickrev[5]), showed patches of high density plasma convecting poleward through the cusp into the polar cap. These observations support the concept of solar produced plasma equatorward of the cusp as the source region of the convecting polar cap patches. Foster and Doupnik[6] presented similar results using dayside measurements from the Chatanika Radar.

This report presents new aspects of polar cap F-layer patches: Total Electron Content (TEC) variations within patches using measurements from the Global Positioning System (GPS) satellites; and observation of patch convection over large distances ($\gtrsim$ 1500 km) using coordinated measurements from Thule and Sondrestrom Greenland. The GPS measurements provide the first quantitative measure of TEC variations within patches, as well as, the first polar cap scintillation measurements at L-band frequencies (1.2 GHz) at high elevation angles. Preliminary results on the operational aspects of GPS measurements at Thule are presented by Klobuchar et al.[7] These coordinated measurements between Thule and Sondrestrom are the first multi-station measurements to show transport of localized regions of enhanced density over large distances in the polar cap.

2. OBSERVATIONS

Measurements described in this report were obtained on 3 and 4 February 1984 from two ground stations; Thule, Greenland (86° CGL) and Sondrestrom, Greenland (75° CGL). The various types of measurements at each location are summarized in Table 1. Magnetic conditions were disturbed with the three hour K_p = 4+, 6 and 5+ during the interval from 3 February 21 UT to 4 February 06 UT.

2.1 Thule Observations

All Sky Imaging Photometer (ASIP) 6300 Å airglow images, shown in Figure 1, define the large scale patch structure observed during this period. These are

(Due to the large number of references cited above, they will not be listed here. See References, page 15.)

similar to other airglow images presented by Weber et al[2] and show a 1200-km diameter circle of the F-region above Thule. The dawn-dusk (06-18) and noon-midnight (12-00) CG Local Time meridians are projected into the 155° field-of-view images to provide a reference frame. The images, at 5-min intervals from 2300 UT 3 February to 0155 UT 4 February 1984, show large scale (up to 1000 km) patches of enhanced 6300 Å airglow drifting in the anti-sunward direction. The all-sky imaging system was actually operated at a rate of one image every 30 sec, and the higher time resolution format clearly shows the continuous anti-sunward drift. Airglow patches were observed until ~0330 UT, although the images are not presented in this report. The main purpose of the images in this study is to identify times when patches drifted through the signal raypaths to two satellites; a high altitude polar beacon satellite transmitting at 250 MHz (raypath shown as a dot in the images), and one of the GPS satellites (raypath shown as a +). The GPS satellites transmit pseudo noise signals at two carrier frequencies from which the ionospheric group delay, proportional to absolute TEC, and amplitude and phase scintillation can be measured. They are in 63° inclination, 12-hour sidereal circular orbits with each satellite visible over Thule for up to four hours. At 0128 UT on 4 February, the GPS receiver was switched to another satellite that was moving to a higher elevation angle, explaining the fast change in position of the GPS location shown between the images at 0125 and 0130 UT in Figure 1.

Table 1. Ionospheric Parameters

Location	System	Measured Parameters
Thule	GPS	TEC, ϕ and amplitude scintillation (1.2 GHz)
	Polar Beacon	ϕ and amplitude scintillation (250 MHz)
	ASIP	Airglow morphology
	Digital Ionosonde	foF2, h'F, and so on
	Vertical Spectrometer	Airglow intensity
Sondrestrom	Incoherent Scatter Radar	N_e, T_e, V_i

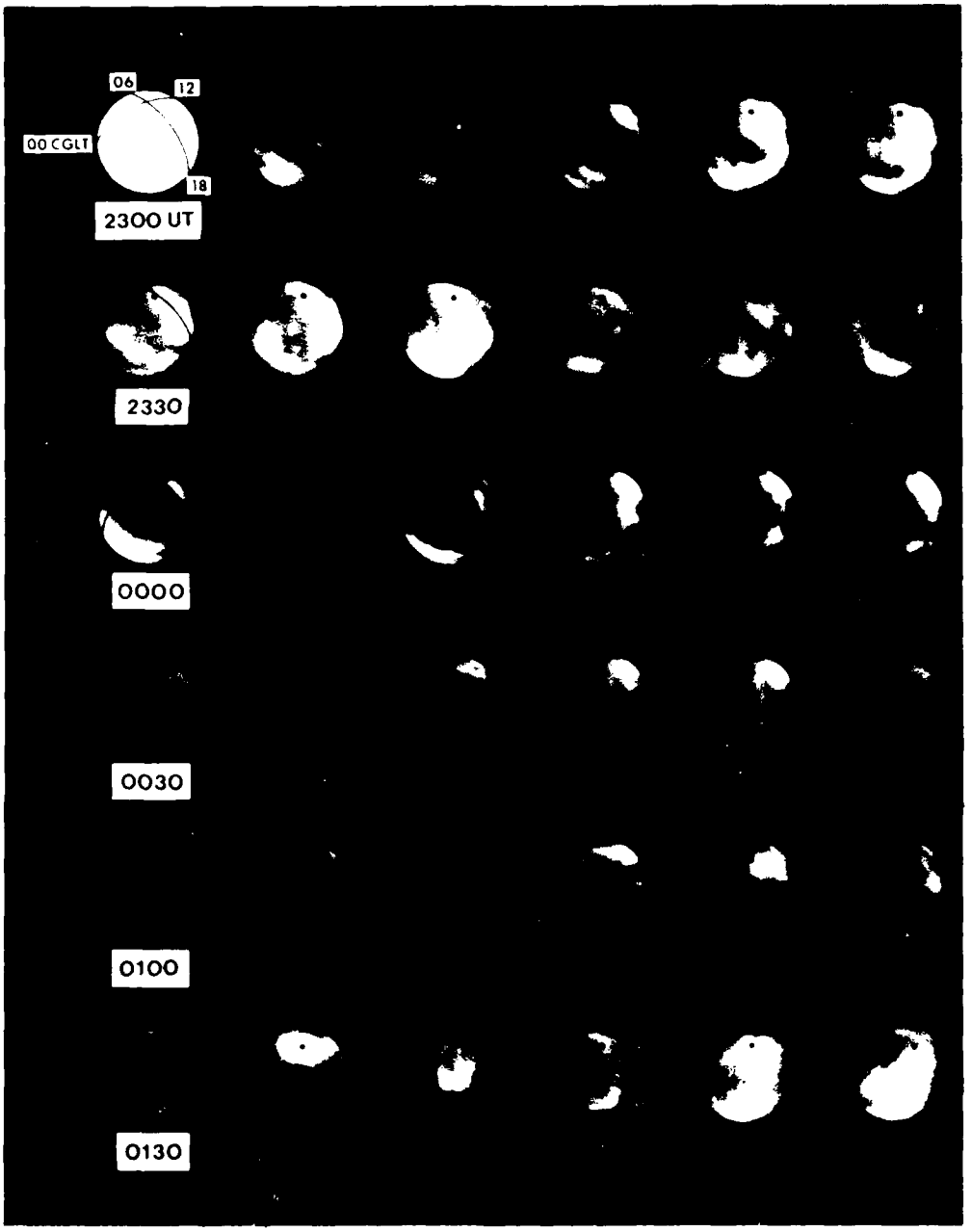

Figure 1. All Sky (155° field of view) 6300 Å Images at Five-min Intervals to Illustrate Large Scale Patch Structure and Drift. The C.G. dawn-dusk and noon-midnight coordinates are projected into the images at a height of 250 km. The E on the circle indicates the location of the zenith to the polar beacon satellite; the N indicates the GPS zenith.

Figures 2a and 2b show the TEC variations and L-band scintillation index (S_4) measured using the GPS downlink. Times when the raypath penetrated an F-region patch, as determined from the optical images, are indicated by shaded bands along the abscissa. The S_4 scintillation index is the normalized variance of the signal intensity (Yeh and Liu[8]) and is a commonly accepted measure of signal fluctuation caused by ionospheric irregularities. In the GPS case, the intensity scintillation is caused primarily by irregularities with spatial wavelengths near 300 m. A comparison of the TEC variations with the raypath location shows a direct association between TEC increases and patch intersection. Patch densities are characterized by increases of 10 to 15 TEC units from quiet background levels of 5 TEC units (1 TEC = 10^{16} el/m^2 column). These increases confirm the earlier results of F-region plasma density enhancements within the patches, determined by digital ionosonde measurements (Buchau et al[3]). Figures 3a and 3b show the foF2, or peak plasma density and 6300 Å zenith airglow intensities at Thule during this period. These measurements confirm large variations in F-region plasma density (background levels $\lesssim 1 \times 10^5$ el/cm^3; peak densities of $\sim 8 \times 10^5$ el/cm^3) and 6300 Å airglow variations during the period 2250 UT 3 February, to 0330 4 February corresponding to the period of the large TEC variations. It is evident that foF2 and TEC enhancements and increases in 6300 Å zenith intensity are different signatures of the same plasma patches. The lack of exact correspondence in time among the three parameters is due to the combined effects of patch size, drift direction, and the off-zenith location of the GPS raypath (for example, 0400 UT).

Figures 2c and 2d show a composite plot of the 250-MHz signal amplitude and the S_4 index. It should be noted that scintillation activity before and after the period shown in the figure was minimal. Generally, there is good agreement between the patch observation and the occurrence of 250-MHz amplitude scintillation that is caused by irregularities of approximately 650-m spatial scale. Up through about 0200 UT, both the optical signatures and the scintillation regions are isolated and distinct, and correlate well with one another. Between about 0200 and 0300 UT, both the scintillation and optical ASIP data suggest a series of patches that largely blur together into a region of irregularly enhanced ionization.

---

8. Yeh, K.C., and Liu, C.H. (1982) Radio wave scintillation in the ionosphere. Proc. IEEE, 70:324.

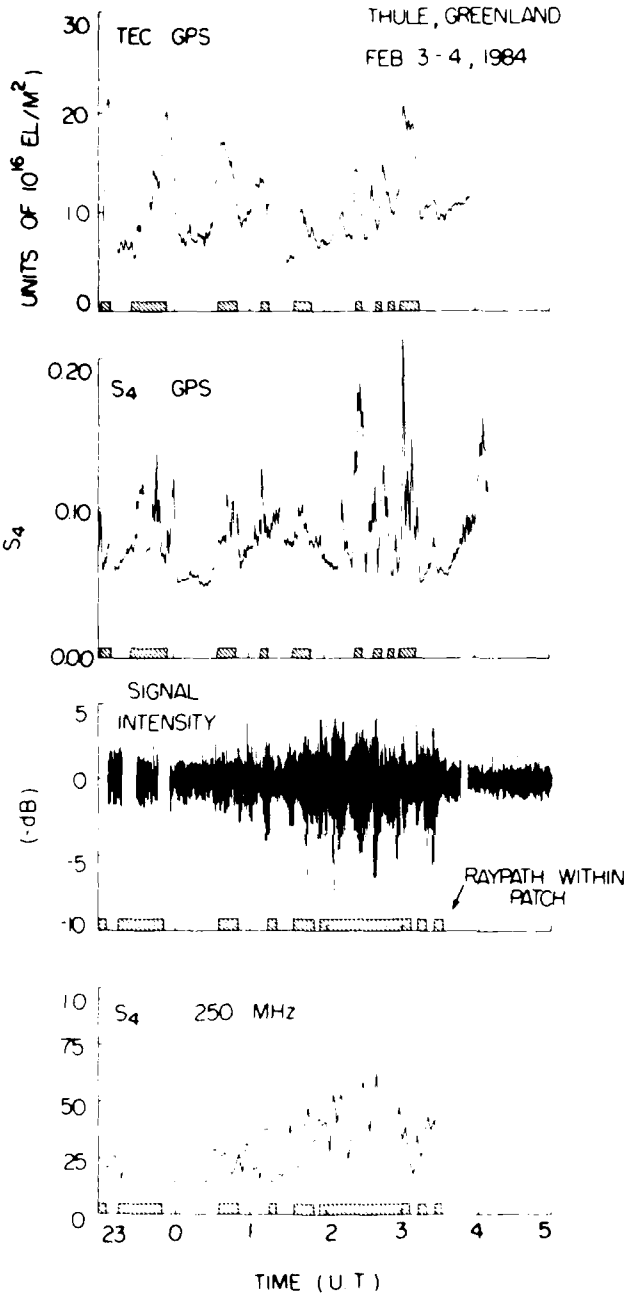

Figure 2. Composite Plot of Total Electron Content (A) and S_4 Index (B) for the GPS Satellite and 250-MHz Signal Strength (C) and S_4 Index (D) for the Polar Beacon Satellite, for the Period 23 UT 3 February to 05 UT 4 February 1984

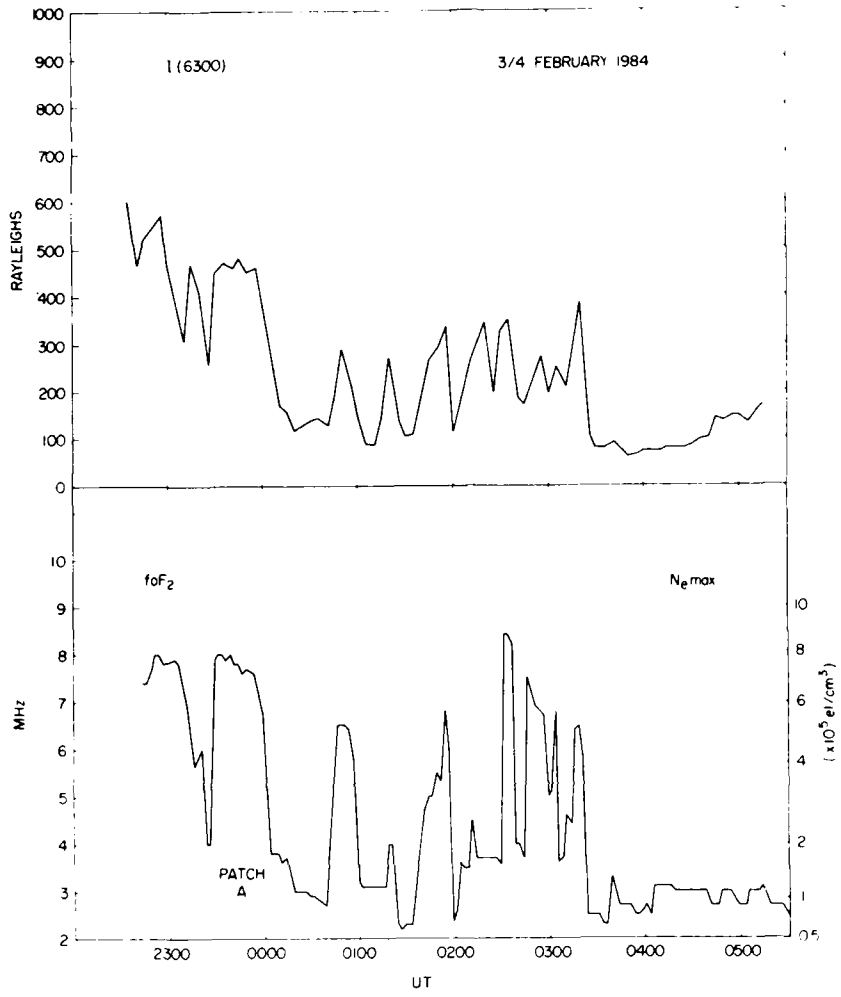

Figure 3. 6300 Å Airglow Zenith Intensity (A) and F-region Peak Density (B) for the Period 23 UT 3 February to 0500 UT 4 February 1984

The correlation between significant enhancement of TEC and the patch images, defined by 6300 Å (recombination) enhancements, is quite good. This is as would be expected, with minor variation in timing that could be due to differences between the electron density profiles and the 6300 Å volume emission rate profiles. The correlation between 6300 Å patches and scintillation enhancements is good but somewhat less distinct. This is also as would be expected because the scintillation depends on both electron content and fluctuations in line-of-sight electron content.

Also of interest is the systematic increase followed by a decrease of the scintillation level during the observation period. This may be a result of either a change in the process producing the kilometer-scale irregularities, or a change in the irregularity anisotropy. Similar changes were measured by Livingston et al[9] near the poleward edge of the auroral oval near midnight.

The final observation from Thule is the relation of L-band amplitude scintillation to TEC variations. This is a significant comparison since it uniquely relates regions of intense ionospheric irregularities of spatial scale equal to approximately 300 m to TEC or bulk plasma density variations using the same raypath. This allows a direct comparison of irregularity intensity, for example, on the leading or tailing edge of the plasma enhancement and may help identify candidate plasma instability mechanisms. Figure 4 shows a detailed comparison of the S_4 scintillation index (top) with TEC (bottom) using the GPS signal. Dashed reference lines are extended from the maxima of the TEC variations for ten distinct events. In cases 3, 7, and 9, there is a clear increase in the S_4 index or irregularity intensity, on the trailing edge of the individual patches, as compared to the S_4 index observed at the leading edge. In all cases, a significant level of scintillation ($S_4 \sim 0.08$) exists within the entire patch, with increases to $S_4 > 0.1$ occurring at the edges. The implication of this comparison is considered further in Section 3.

2.2 Sondrestrom Observations

During the period covering the above discussed observations, the Sondrestrom Incoherent Scatter Radar was operated in a multiposition mode to provide latitude/local time maps of electron density, temperatures and ion drifts over the range from 70° to ~80° CGL, with a cycle time of ~16 minutes. In addition, east-west magnetic meridian scans were performed at 52-min intervals. Figures 5a and 5b show electron density maps for the period 0840 UT 3 February to 0758 UT 4 February for 277 and 200 km altitude. Universal Time is indicated on the inside dial, local time on the outside dial.

---

9. Livingston, R. C., Tsunoda, R. T., Vickrey, J. F., and Guerin, L. (1985) of high latitude nighttime F-region irregularities, J. Geophys. Res., 87:10519.

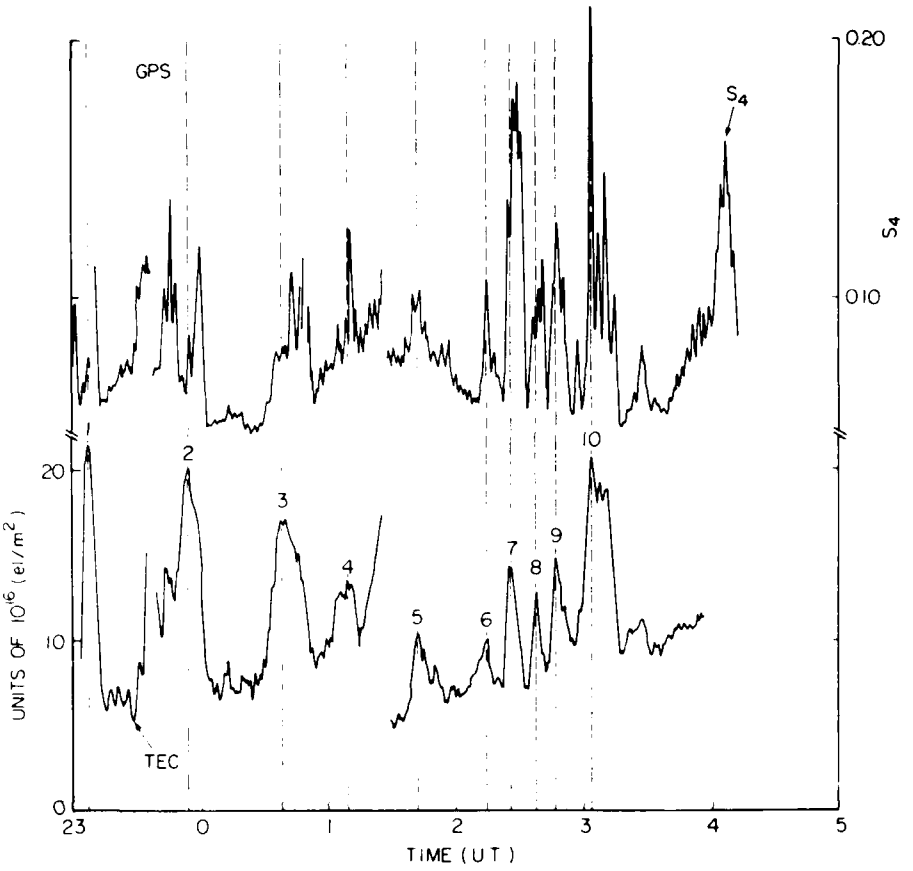

Figure 4. Detailed Comparison of GPS TEC and S_4 Variations

The poleward edge of the Sondrestrom radar field of view is close to the equatorward edge of the Thule ASIP field of view. The altitude of 277 km was selected for the density and temperature plots of Figure 5a and 5c because it corresponds to the autocorrelator gate closest to the F-layer peak. The Sondrestrom radar measurements of electron density profiles showed that this peak was between 280 and 310-km altitude.

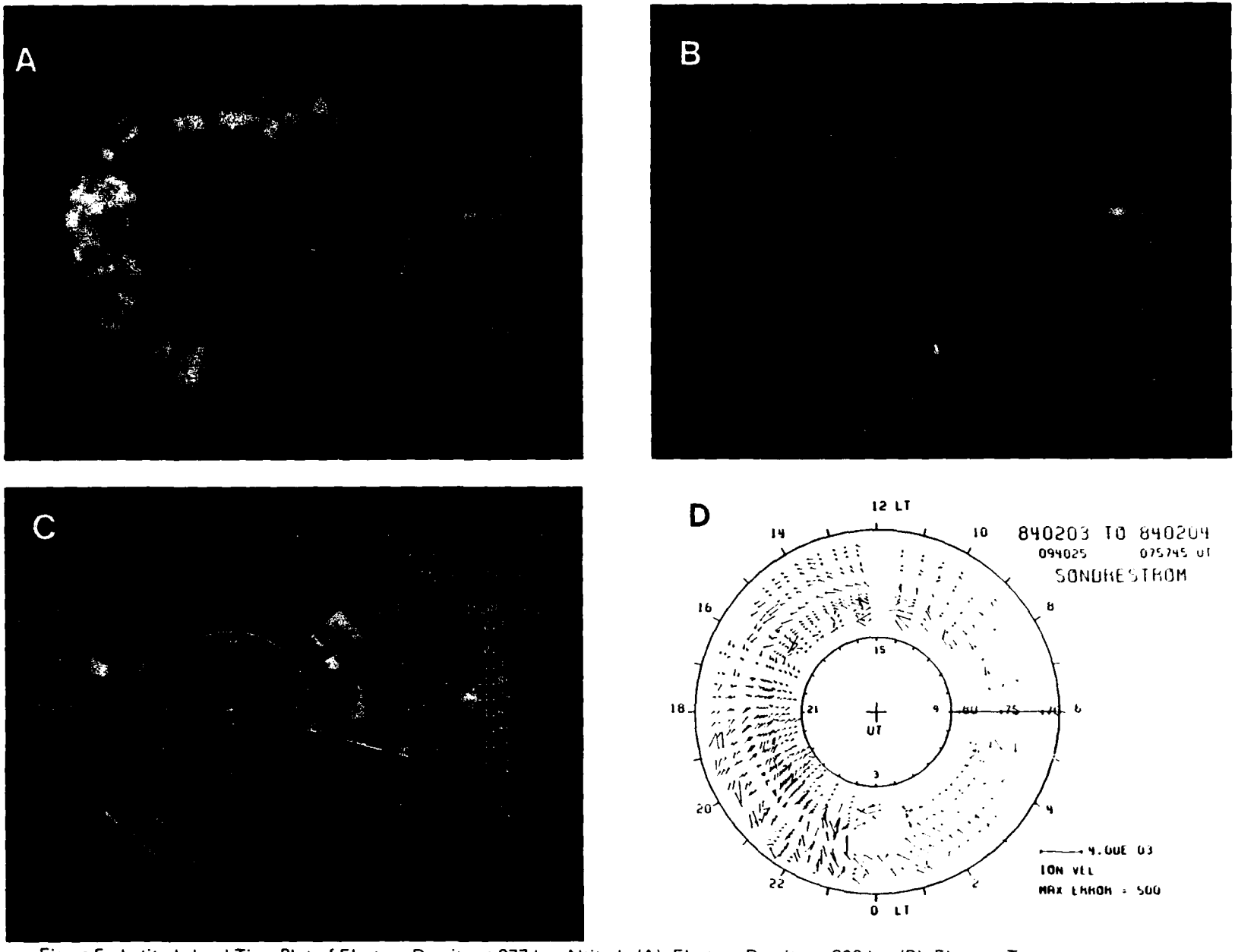

Figure 5. Latitude-local Time Plot of Electron Density at 277 km Altitude (A), Electron Density at 200 km (B), Electron Temperature at 277 km (C), and Ion Drift Velocity (D) Measured by the Sondrestrom Incoherent Scatter Radar on 3 and 4 February 1984

Of direct interest to this study is the increase in electron density (to $\sim 3.5 \times 10^5$ el/cm^3) at 277-km altitude after 2300 UT on 3 February. The increase appears first at the highest latitudes and fills the entire coverage area by 0300 UT. These enhanced densities are, in fact, the dominant F-region density feature for the entire 24-hr period of Sondrestrom observations. The combined electron density and ion drift velocity measurements indicate the flow of a region of enhanced F-region plasma from the vicinity of Thule toward Sondrestrom during a period of limited duration. From 2100 UT to 0115 UT the ion drift velocities (Figure 5d) were mostly southward; they progressively turned from a southeast to a southwest direction. At 0000 UT they were almost parallel to the direction from Thule to Sondrestrom. Local time at Thule is 1 hr behind Sondrestrom, therefore, in Figure 5d flow from Thule to Sondrestrom would be generally southward with a small easterly component. The flow started to intensify at 0015 UT and, by 0130, the flow velocity had almost doubled. The magnetograms from the Greenland chain show increased activity at 0015 UT, with a maximum ΔH negative bay of 900 γ at 67.5° CGL, reached at 0050 UT. The change in the electric field pattern commencing at 0015 UT may have been associated with this substorm activity. The period when patches of enhanced densities are observed ends at 0115 UT, approximately two hours earlier than at Thule. The last patch appeared only in the northernmost beam position (Figure 5a), in a region of westward flow. This patch corresponds to the patch observed overhead Thule from 0045 to 0055 UT. Subsequent patches observed with the ASIP at Thule drifted southwest, and did not pass through the Sondrestrom radar field of view. This is confirmed by the change in flow direction observed at Sondrestrom after 0115 UT. The change in flow direction (westward poleward of the station, and eastward equatorward of the station) suggests that the radar rotated into the dawn convection cell at this time. Convection within this cell may not necessarily transport flux tubes from the same high density source region, which may explain the absence of high density plasma at the radar after 0115 UT.

The electron density map at 200-km altitude (Figure 5b) and the electron temperature map (Figure 5c) reveal two important features: while the 277-km density enhancement was not characterized by a corresponding increase in electron temperature, the density increases seen to the south in the 200-km map at later times (0030 to 0630 UT) were clearly associated with electron temperature increases. These density increases at 200-km altitude, with corresponding elevated T_e that reached 2300° K, are due to direct production by precipitating auroral zone particles in this region. They are associated with the substorm activity mentioned above.

During the one and three-quarter hour period that the patches were in the Sondrestrom radar field of view, the electron temperature showed no measurable enhancement, thereby establishing negligible particle precipitation and local production. The presence of particle precipitation adequate to lead to any appreciable ionization production would have simultaneously manifested itself in readily measurable heating of the electron gas. Thus, the long time history of unenhanced electron temperature (at 277 km) in the patches is direct evidence of transport of non-locally produced F-region plasma into the Sondrestrom field of view from the direction of the central polar cap, and is consistent with the optical intensities of the patch at Thule which did not show evidence of particle precipitation (that is, lack of N_2^+(0-0) radiation at 3914 Å).

An important feature is the absence of significant density increases at 277 km associated with particle precipitation in the nightside auroral zone that has recently received considerable attention (Robinson et al;[10] Weber et al;[11] and de la Beaujardiere et al[12]). The present observations indicate that high altitude F-region patches can be transported from the polar cap into the oval, and that patches are not produced by auroral zone precipitation, as proposed by Robinson et al, [10] but rather are convected across the polar cap into the auroral zone as proposed by Weber et al[11] and de la Beaujardiere et al. [12] Furthermore, the UT period when the patches are observed is consistent with the conclusions reached by de la Beaujardiere et al. [12] These authors showed that, due to the displacement of the geographic and geomagnetic poles, the nighttime F-region density depends strongly on Universal Time. Patches of ionization were regularly seen in the polar cap and midnight auroral zone, within the 2000 to 0200 UT period, when the solar illumination of the auroral oval covers the largest area.

Attention is now focused on one patch in this data set to explicitly track it from Thule through Sondrestrom. The foF2 enhancement over Thule from 2325 to 0000 UT, marked "A" in Figure 3, is readily identified in Figure 1 as a bright, structured patch. The leading edge of this patch passes across the center of the ASIP at 2320 UT, and the trailing edge overhead at 2355 UT. The foF2 and TEC data (Figures 3 and 4) are consistent with the optical observations. As determined

---

10. Robinson, R. M., Tsunoda, R. T., Vickrey, J. F., and Guerin, L. (1985) Sources of F-region ionization enhancements in the nighttime auroral zone, J. Geophys. Res., 90:7533.

11. Weber, E. J., Tsunoda, R. T., Buchau, J., Sheehan, R. E., Strickland, D. J., Whiting, W., and Moore, J. G. (1985) Coordinated measurements of auroral zone enhancements, J. Geophys. Res., 90:6497.

12. de la Beaujardiere, O., Caudal, C., Holt, J., Craven, J., Wickwar, V. B., Brace, L., Evans, D., Winningham, J. D., and Heelis, R. A. (1985) Universal time dependence of nighttime F-region densities at high latitudes, J. Geophys. Res., 90:4319.

from the ASIP measurements, the velocity of this patch of enhanced density is anti-sunward, at ~550-600 m/sec, on a track which leads straight toward Sondrestrom. The patch diameter is estimated to be ~1200 km from the ASIP image.

In Figure 5a, the Sondrestrom radar is 1200 km south of Thule, and the poleward edge of the radar field of view (78.2° CGL) is 700 km south of Thule. Given these distances, patch dimension and velocity (550-650 m/sec from the ASIP, 500-550 m/sec from the radar), Patch A should enter the northern edge of the radar field of view at 2341 UT, reach the radar zenith at 2356 UT, and be centered over the radar at 0014 UT. This is observed as the region of highest electron density in Figure 5a, that extends over the full Sondrestrom field of view at 0015 UT. Although not shown in this report, close examination of the densities in the individual beam positions clearly shows the southward motion of this patch. Density increases are observed at beam positions north, overhead and south of the radar within ~1 min of the postulated nominal arrival times. Enhanced density regions are seen at the northern edge of the radar field of view as early as 2310 UT. These are related to smaller patches that are seen to drift out of the southern edge of the ASIP toward the radar at this earlier time.

A radar E-W elevation scan took place from 0010 and 0015 UT, when Patch A was roughly centered above the radar. This scan shows that this F-region density enhancement was fairly structured and that its E-W dimension was ~900 km. This dimension is similar to that inferred from the Thule all-sky imaging photometer observations. The foF2, TEC and ISR data further show quantitative consistency. The ionosonde measured sustained enhanced peak electron densities of 8×10^5 cm^{-3} inside the patch, and 2×10^5 cm^{-3} outside the patch. Taking the equivalent slab thickness of 250 km determined from the density profile measured downstream by Sondrestrom, this should lead to an electron content within and outside the patch of 20 TEC units and 5 TEC units respectively. This compares extremely well with the observed value of 20 TEC units within the patch against a background of about 6 TEC units. The ISR measured the patch downstream from Thule and about one-half hour later. It is still enhanced by a factor of 3.5 to 4 over the background, with a peak density near 4×10^5 el/cm^{-3} against a background near 1×10^5 el/cm^{-3} Thus, the densities in both the patch and background have decreased by a factor of two over the 40 min separating the measurements. This is in good agreement with commonly accepted F-region decay rates due to recombination.

Therfore, the combined Thule and Sondrestrom data show a large ionization patch drifting through the Thule and then through the Sondrestrom fields of view. This is the first direct tracking of an ionospheric patch from the CG pole to ~70° CGL, a total distance of ~3300 km.

3. DISCUSSION

These observations present further characteristics of the structure and transport of F-region patches in the polar cap, and their relation to smaller scale (< 1 km) ionospheric irregularities. During disturbed magnetic conditions, a limited period of patch transport over the polar cap and into the nightside auroral zone was clearly observed. The most significant new results are quantitative measurements of TEC enhancements of 10 to 15 TEC units above a background of five TEC units associated with the patches, and the ability to associate irregularity intensity with specific regions within the patches through simultaneous (and coincident) TEC and L-band scintillation measurements. Comparison shows a systematic increase in amplitude scintillation on the trailing edge of several patches. This is the E × B unstable side of the patch, assuming Vion > Vneutral, and reconfirms earlier observations by Weber et al.[2] Equally important are the levels of scintillation on the leading edge and throughout the interior of the patches. Evidence for internal structures within patches was shown by Buchau et al[3] using digital ionosonde measurements. Lee[13] has proposed that thermal effects (Ohmic dissipation of Pedersen current) due to the dc (or convection) electric field can give rise to ionospheric irregularities throughout the interior of convecting F-region patches. This is an attractive candidate process, since it depends only on a threshold dc electric field of $\gtrsim$ 25 mv/m (corresponding to convection velocities of $\gtrsim$ m/s), conditions readily satisfied by the measurements presented in this report. The observations establish a combination of plasma destabilizing effects in the patch; and are consistent with E × B on the trailing edge, and thermal effects operating within the plasma patches as described in the theoretical calculations of Lee.[13] Other mechanisms which could lead to structuring within the patches have been proposed by Fejer and Kelley.[14]

Observations at Sondrestrom confirm that the plasma patches convect out of the polar cap and into the high latitude region of the auroral oval. Recent measurements of F-region plasma "blobs" on the equatorward edge of the auroral oval (Weber et al[11]) indicate a non-local source region for these features. These Sondrestrom radar observations, in combination with the multisensor patch observations at Thule, support the concept of cross polar cap transport as a source for nightside auroral zone F-region plasma.

---

13. Lee, M. C. (1985) Contributions of thermal effects to occurrence of irregularities in the high latitude ionosphere, Radio Sci. (submitted).

14. Fejer, B. G., and Kelley, M. C. (1980) Ionospheric Irregularities, Reviews of Geophys. and Space Phys., 18:401.

Future measurements are planned to trace individual plasma patches, and to measure the irregularity spectrum using scintillation measurements at each location. This will provide valuable insight into the scale size dependence of the evolution of the irregularity spectrum under reasonably well-known conditions.

References

1. Buchau, J., Reinisch, B.W., Weber, E.J., and Moore, J.G. (1983) Structure and dynamics of the winter polar cap F Region, Radio Sci., 18:995.

2. Weber, E.J., Buchau, J., Moore, J.G., Sharber, J.R., Livingston, R.C., Winningham, J.D., and Reinisch, B.W. (1984) F-layer ionization patches in the polar cap, J. Geophys. Res., 89:1683.

3. Buchau, J., Weber, E.J., Anderson, D.N., Carlson, H.C., Jr., Moore, J.G. Reinisch, B.W., and Livingston, R.C. (1985) Ionospheric structures in the polar cap: their origin and relation to 250-MHz scintillation, Radio Sci., 20:325.

4. Weber, E.J., and Buchau, J. (1985) Observation of Plasma Structure and Transport at High Latitudes, the Polar Cusp, J.A. Holtet and A. Egeland, Eds., Reidel Publishing Co., p. 279.

5. Kelly, J.D., and Vickrey, J.F. (1984) F-region ionospheric structure associated with anti-sunward flow near the dayside cusp, Geophys. Res. Lett., 11:907.

6. Foster, J.C., and Doupnik, J.R. (1984) Plasma convection in the vicinity of the dayside cleft, J. Geophys. Res., 89:9107.

7. Klobuchar, J.A., Bishop, G.J., and Doherty, P.H. (1985) Total Electron Content and L-Band Amplitude and Phase Scintillation Measurements in the Polar Cap Ionosphere, Proc. NATO AGARD Electromagnetic Wave Panel Symp: Propagation Effects on Military Systems in High Latitude Regions, Paper 2-2, 3-7 Jun, Fairbanks, Alaska.

8. Yeh, K.C., and Liu, C.H. (1982) Radio wave scintillation in the ionosphere, Proc. IEEE, 70:324.

9. Livingston, R.C., Rino, C.L., Owen, J., and Tsunoda, R.T. (1982) Anisotropy of high latitude nighttime F-region irregularities, J. Geophys. Res., 87:10519.

10. Robinson, R.M., Tsunoda, R.T., Vickrey, J.F., and Guerin, L. (1985) Sources of F-region ionization enhancements in the nighttime auroral zone, J. Geophys. Res., 90:7533.

References

11. Weber, E.J., Tsunoda, R.T., Buchau, J., Sheehan, R.E., Strickland, D.J., Whiting, W., and Moore, J.G. (1985) Coordinated measurements of auroral zone enhancements, J. Geophys. Res., 90:6497.

12. de la Beaujardiere, O., Caudal, C., Holt, J., Craven, J., Wickwar, V.B., Brace, L., Evans, D., Winningham, J.D., and Heelis, R.A. (1985) Universal time dependence of nighttime F-region densities at high latitudes, J. Geophys. Res., 90:4319.

13. Lee, M.C. (1985) Contributions of thermal effects to occurrence of irregularities in the high latitude ionosphere, Radio Sci. (submitted).

14. Fejer, B.G., and Kelley, M.C. (1980) Ionospheric Irregularities, Reviews of Geophys. and Space Phys., 18:401.

END

2-87

DTIC